Theory of anisotropic whispering-gallery-mode resonators

Marco Ornigotti[1,*] and Andrea Aiello[1,2]

[1]*Max Planck Institute for the Science of Light, Günther-Scharowsky-Strasse 1/Bau24, D-91058 Erlangen, Germany*
[2]*Institute for Optics, Information and Photonics, University of Erlangen-Nuernberg, Staudtstrasse 7/B2, D-91058 Erlangen, Germany*

An analytic solution for a uniaxial spherical resonator is presented using the method of Debye potentials. This serves as a starting point for the calculation of whispering gallery modes (WGMs) in such a resonator. Suitable approximations for the radial functions are discussed in order to best characterize WGMs. The characteristic equation and its asymptotic expansion for the anisotropic case is also discussed, and an analytic formula with a precision of the order $O[\nu^{-1}]$ is also given. Our careful treatment of both boundary conditions and asymptotic expansions makes the present work a particularly suitable platform for a quantum theory of whispering gallery resonators.

I. INTRODUCTION

London's St. Paul's Cathedral is famous for its rich history and architecture; one of the most unique aspects of this building is the whispering gallery that runs along the interior wall of its dome [1]. When sounds are uttered in low voice against the wall, sound waves generated circulate around the wall many times before fading away. As these waves propagate, they bring with them sounds that are audible on the opposite side of the dome. On the contrary, if the same sounds are uttered at higher volume, the frequencies of these sound waves will not match and a lot of noise is created, making the message difficult to be heard at any part of the wall.

The physical explanation of this effect was first given more than a century ago in terms of reflection of acoustic *rays* from a surface near the dome apex. It was initially assumed that the rays that propagate along different large arcs of the dome in the form of a hemisphere should concentrate only at the point diametrically opposite to the source of the sound. Afterwards lord Rayleigh, in his theory of sound [2], provided a different explanation of the effect that he named whispering gallery waves: sound clutches to the wall surface and creeps along it without diverging as fast as during the free space propagation—these sound waves then propagate within a narrow layer adjacent to the wall surface. It was then discovered, at the beginning of the last century, that optical whispering gallery waves can exist even in dielectric spheres [3,4]. An optical resonator that shows this particular wave structure was then called a whispering gallery resonator (WGR). In recent times whispering gallery waves have found new fame with the development of nano-optics, in particular with the ability to manufacture spherical and toroidal WGRs with very high quality factors that range from 10^7 to 10^{10} [5–7]. This motivated a large theoretical and experimental work around these devices (see, for example, Refs. [8–11], and references therein). The ability to store light in microscopic spatial volumes for long periods of time (due to the high Q factor) resulted in a significant enhancement of nonlinear interactions of various kinds like four-wave mixing [12,13],

Raman [14], parametric and Brillouin scattering [11,15], microwave up-conversion [16], and second- and third-order harmonic generation [17–19]. Besides the field of nonlinear optics, WGRs were recently used even for cavity QED experiments [20,21]. For an exhaustive review on the applications of WGRs, see Ref. [22].

Since many of the applications of these resonators involve nonlinear optics, WGRs are commonly fabricated using nonlinear materials or anisotropic crystals [11]. Despite the wide scientific production in the theory of anisotropic spherical resonators that ranges from generalization of scattering methods [23–26], potential method [27], dyadic Green-function approach [28], and Fourier-based analysis [29], and even though an extensive study of isotropic WGRs was done in the past [30], detailed studies on anisotropic WGRs are still very few. To the knowledge of the authors, anisotropic WGRs are mainly reported in literature as studied with finite-difference time-domain (FDTD) models [31,32], cavity loading [33], and direct solution of Maxwell's equation with a surface nonlinear polarization as a forcing term [10].

In this work, we intend to develop a suitable analytic theory for WGRs, starting from a review of the solutions of Maxwell's equations in a uniaxial spherical resonator, then presenting and discussing its mode structure in the limit of small anisotropy, and finally obtaining the spectrum of whispering gallery modes sustained by the resonator and their structure, discussing how anisotropy influences those modes. A detailed discussion on the application of boundary conditions to this resonator is also presented, pointing out how to apply correctly these conditions and discussing some of their basic features that, to the knowledge of the authors, is not present in earlier works. It is the opinion of the authors that this discussion is important in order to better understand the physics behind this problem. This is the first main result of this work. Finally, we introduce a more accurate approximation for the field outside the resonator when the index of the Hankel function tends to infinity, as we noticed that the commonly used power expansion (as, for example, the one presented in Ref. [30]) does not match the exact function completely, i.e., it has an additional phase factor with respect to the real function. Such a phase factor becomes relevant when field amplitude, as opposed to field intensity, turns out to be fundamental. This happens, for example, when

---

*marco.ornigotti@mpl.mpg.de

one wants to quantize the electromagnetic field inside the resonator, as required for a proper treatment of spontaneous emissions processes. Thus the present work may serve as a basis for a quantum theory of WGRs. This is the second main result of this work.

This paper is organized as follows: in Sec. II the Debye method of potentials for solving Maxwell's equations is briefly presented and then used in Sec. III to develop the theory of an anisotropic spherical resonator for a dielectric uniaxial sphere. In Sec. IV, whispering gallery modes (WGMs) are obtained as a limiting case of the normal modes of the dielectric sphere with high quantum numbers, and their spectrum is discussed.

II. ISOTROPIC SOLUTIONS

A. Solution to Maxwell's equations in spherical coordinates

Let us consider a monochromatic field with a harmonic time dependence [i.e., $\vec{E}(\vec{x},t) = \vec{E}(\vec{x})e^{-i\omega t}$] in an isotropic sourceless spherical dielectric medium characterized by a dielectric constant ε, a radius R, and surrounded by air. The set of Maxwell's equations in spherical coordinates can be written in the following compact form:

$$\frac{\partial}{\partial \zeta_n}(L_m E_m) - \frac{\partial}{\partial \zeta_m}(L_n E_n) = -ik\epsilon_{lnm}L_n L_m H_l, \quad (1a)$$

$$\frac{\partial}{\partial \zeta_n}(L_m H_m) - \frac{\partial}{\partial \zeta_m}(L_n H_n) = ik\epsilon_{lnm}L_n L_m E_l, \quad (1b)$$

where $\{l,n,m\} \in \{1,2,3\}$, ζ_m are the spherical coordinates ($\zeta_1 = \varphi$, $\zeta_2 = \theta$ and $\zeta_3 = r$), L_m are the metric coefficients of the spherical reference frame ($L_1 = r \sin\theta$, $L_2 = r$, $L_3 = 1$), and ϵ_{lnm} is the Levi-Civita symbol. For the sake of simplicity, let us fix our attention on TM waves (i.e., those having $H_r = 0$); the calculations for TE waves can be straightforward obtained by analogy.

By introducing the TM potential U, the solution to Eqs. (1) can be easily found with the standard method of Debye potentials [34] and reads

$$U_{nm}^{int/ext}(r,\theta,\varphi) = C_{int/ext}\sqrt{kr}Z_\nu(kr)Y_{nm}(\theta,\varphi), \quad (2)$$

where $\nu = n + 1/2$, n,m are the angular quantum numbers that address the single mode of the resonator, $Z_\nu(kr)$ is the radial Bessel-type function that is equal to the Bessel function $J_\nu(kr)$ inside the dielectric sphere (where the solution has to be finite at the origin), and is equal to the Hankel function of the first kind $H_\nu^{(1)}(k_0 r)$ outside the dielectric sphere, where the solution has the general form of a traveling wave in order to fulfill the Sommerfeld radiation condition.

The constants $C_{int/ext}$ are to be determined by applying suitable boundary conditions. Note that the argument of the Bessel function inside the sphere contains the sphere dielectric constant ε via the wave vector $k = \omega\sqrt{\varepsilon}/c$ while the argument of the Hankel function outside the sphere contains only the vacuum wave vector $k_0 = \omega/c$ because $\varepsilon_{air} = 1$.

The components of the electric and magnetic fields for TM waves can then be written as a function of U as follows:

$$E_r = \left(\frac{\partial^2}{\partial r^2} + k^2\right)U, \quad H_r = 0, \quad (3a)$$

$$E_\theta = \frac{1}{r}\frac{\partial^2 U}{\partial r\partial\theta}, \quad H_\theta = -ik\frac{1}{r}\frac{\partial U}{\partial\varphi}, \quad (3b)$$

$$E_\varphi = \frac{1}{r\sin\theta}\frac{\partial^2 U}{\partial r\partial\varphi}, \quad H_\varphi = ik\frac{1}{r}\frac{\partial U}{\partial\theta}. \quad (3c)$$

Similar expressions can be found for TE waves [34].

B. Boundary conditions

Prior to investigating the structure of the modes for the anisotropic resonator, it is important to discuss the boundary conditions that have to be applied to this problem. At the resonator surface $r = R$, the wave vector k inside the dielectric sphere has to match the wave vector $k_0 = \omega/c$ outside the sphere and the constants C_{int} and C_{ext} should be chosen properly.

There is not a unique way to fulfill boundary conditions: in fact, one could apply "pure" or "mixed" conditions: the former consists in applying the boundary conditions to all the components of only electric *or* magnetic field, while the latter applies the boundary to certain components of one field and certain other components of the other field. Obviously, these two different paths bring us to the same physical solutions [34]. Among these possibilities, in this work we chose to apply "pure" boundary condition, i.e., we impose that the tangential electric (magnetic) -field components for TM (TE) waves have to be continuous at the resonator surface $r = R$, while the radial component of the displacement vector $\vec{D} = \varepsilon\vec{E}$ is continuous across the resonator surface. For TE fields, the radial condition is automatically fulfilled, since the resonator is nonmagnetic (i.e., $\mu = 1$).

The condition for the radial component of the displacement vector ($\varepsilon_{int}E_r^{int} = \varepsilon_{ext}E_r^{ext}$) across the resonator surface gives the ratio between the inner and outer coefficients, while the continuity of the tangential component $E_{\theta,\varphi}^{int} = E_{\theta,\varphi}^{ext}$ of the field gives rise to the so-called characteristic equation, that allows us to determine the allowed values for the wave vector k (i.e., to find the spectrum of the allowed modes) inside the resonator, and it turns out to be

$$\frac{[j_\nu(kR)]'}{j_\nu(kR)} = \sqrt{\varepsilon}\frac{\left[h_\nu^{(1)}(k_0 R)\right]'}{h_\nu^{(1)}(k_0 R)}, \quad (4)$$

for TM waves. The TE-characteristic equation is simply obtained by replacing $\sqrt{\varepsilon}$ with $1/\sqrt{\varepsilon}$. In these equations $j_\nu(x) = \sqrt{x}J_\nu(x)$ and $h_\nu^{(1)}(x) = \sqrt{x}H_\nu^{(1)}(x)$ are the Riccati-Bessel functions, and the prime indicates the total derivative with respect to their arguments. Although formally corrected, as they are these boundary conditions do not provide a unique solution to the determination of the mode patterns in the resonator.

In order to better understand this nonuniqueness of the solution, let us consider the general structure of Eq. (4). Let $T(x)$ be a piecewise function defined across an interface, placed at $x = 1$, between two regions of space, such that $T(x) = C^{(i)}f(x)$ for $x < 1$ and $T(x) = C^{(e)}g(x)$ for $x > 1$, with $f(x)$ and $g(x)$ two arbitrary real valued and regular functions. The constants $C^{(i,e)}$ are to be determined by the

boundary conditions and they must be chosen in such a way that the following characteristic equation is satisfied:

$$\frac{f'(x)}{f(x)} = \alpha \frac{g'(x)}{g(x)}, \qquad (5)$$

where the apex stands for the derivative of the two functions with respect to their arguments. Since this is a generalization of the characteristic equations (4), it must hold at the interface between the two region of space considered, i.e., its validity is limited to $x = 1$. From Eq. (5) it is clear that if we admit that the derivatives $f'(x)$ and $g'(x)$ of the functions are equal at the separation interface $x = 1$, then the functions themselves will be discontinuous with a jump that has the value of $1/\alpha$. On the other hand, if we now admit that the the functions $f(x)$ and $g(x)$ are equal at the separation interface $x = 1$, then their derivatives must be discontinuous, and the magnitude of the discontinuity is precisely α.

The first situation corresponds to require that the derivative of the function $T(x)$ is continuous at the separation interface [i.e., $T'(1)^+ = T'(1)^-$, where the plus or minus superscript stands for the expression of $T(x)$ for $x > 1$ and $x < 1$, respectively]. This implies that $C^{(e)}/C^{(i)} = f'(1)/g'(1)$ and the function $T(x)$ can be written as

$$T(x) = \begin{cases} f(x), & x < 1, \\ \left[\frac{f'(1)}{g'(1)}\right]g(x), & x \geqslant 1. \end{cases}$$

It is then clear that taking $T'(x)$ to be continuous at the interface results in a discontinuity in the behavior of $T(x)$ while passing through $x = 1$, whose magnitude is $f'(1)/g'(1)$, as is depicted in Fig. 1.

Conversely, the second condition on the functions $f(x)$ and $g(x)$ implies that the function $T(x)$ to be continuous at the separation interface [i.e., $T(1)^+ = T(1)^-$], we have
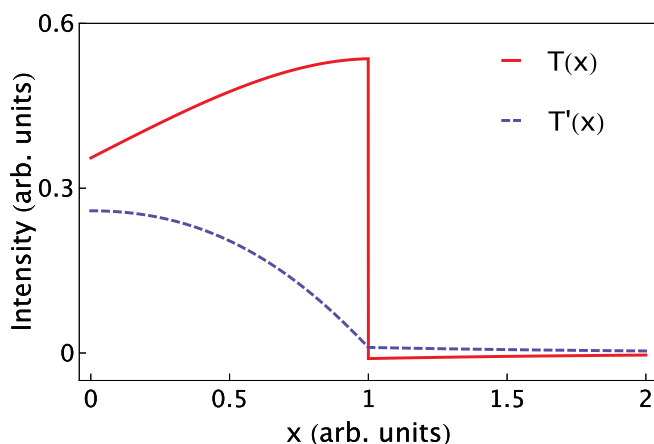
FIG. 1. (Color online) The figure shows the behavior of the function $T(x)$ (red solid line) and its derivative $T'(x)$ (blue dashed line) when the condition of continuous derivative at the separation interface $x = 1$ is considered. As can be noted, in this case the function shows a discontinuity while its derivative is (obviously) continuous. For this example we have used $f(x) = \mathrm{Ai}(x)$ and $g(x) = e^{-x}$, and the magnitude of the discontinuity in the function $T(x)$ at the separation interface is $f'(1)/g'(1) \simeq 0.5457$.
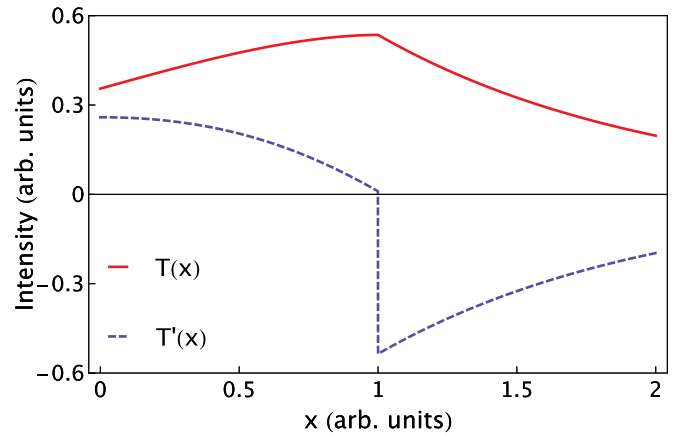
FIG. 2. (Color online) The figure shows the behavior of the function $T(x)$ (red solid line) and its derivative $T'(x)$ (blue dashed line) when the condition of continuous function at the separation interface $x = 1$ is considered. As can be noted, in this case the function itself is (obviously) continuous while its derivative shows a jump discontinuity. For this example we have used $f(x) = \mathrm{Ai}(x)$ and $g(x) = e^{-x}$ and the magnitude of the discontinuity in the derivative $T'(x)$ at the separation interface is $f(1)/g(1) \simeq 0.5457$.

$C^{(e)}/C^{(i)} = f(1)/g(1)$ and the function $T(x)$ has the following form:

$$T(x) = \begin{cases} f(x), & x < 1, \\ \left[\frac{f(1)}{g(1)}\right]g(x), & x \geqslant 1. \end{cases}$$

In this case, taking $T(x)$ to be continuous at the interface results in a discontinuity in its derivative, whose magnitude is $f(1)/g(1)$, as Fig. 2 underlines.

In both cases, however, it is not possible to make the functions *and* the derivatives both continuous at the same time. This fact makes it only possible to obtain the ratio between the two constants C_{int}, C_{ext} and not their explicit value: in order to do that, another condition must be applied to the problem. This condition depends on the particular problem we are dealing with; in scattering problems, for example, the incoming field is known, and determines the field pattern on the resonator surface. In this case C_{ext} is known and the ambiguity is removed. Another situation in which the ambiguity is overcome is by embedding the whole system (resonator plus surrounding medium) in an ideal perfectly reflective sphere of big, but finite radius R_0, in such a way that the boundary conditions at the metallic surface will completely determine the fields: this second approach is very useful if we are dealing with the quantization of the field in such a system.

We want to end this discussion by pointing out that the first situation (derivative continuous at the interface) corresponds to the boundary condition for the electric field across a dielectric surface: the normal component with respect to the separation surface is discontinuous by a factor equal to the ratio of the two dielectric constants of the two regions, while the tangential components (i.e., the derivative of the radial field in our spherical case) are continuous at the interface. The second situation, instead, corresponds to making continuous the normal component of the displacement vector across the separation surface, resulting in a discontinuity of the tangential component of the displacement vector at the interface. While

the former situation corresponds to the usual way of imposing boundary conditions in an electromagnetic problem, the latter is never used, but still valid.

In this work, however, we are neither interested in scattering problems nor in field quantization, and so in the rest of the paper this ambiguity will not be removed. This does not create too many problems because we are only interested on the mode structure of the resonator. We leave this problem of nonuniqueness to future works.

III. NORMAL MODES OF A UNIAXIAL SPHERICAL RESONATOR

Let us consider the same dielectric spherical resonator of radius R of the previous section, but with a uniaxial anisotropy along the z axis described by the following dielectric tensor:

$$\hat{\varepsilon} = \begin{pmatrix} \varepsilon_{xx} & 0 & 0 \\ 0 & \varepsilon_{xx} & 0 \\ 0 & 0 & \varepsilon_{zz} \end{pmatrix}$$
$$= \varepsilon_{xx}(\hat{\mathbf{x}}\hat{\mathbf{x}} + \hat{\mathbf{y}}\hat{\mathbf{y}}) + \varepsilon_{zz}\hat{\mathbf{z}}\hat{\mathbf{z}}. \tag{6}$$

In order to use this dielectric tensor in Eqs. (1), it should be converted in spherical coordinates; this operation is simply done by converting the Cartesian dyadics $\hat{\mathbf{x}}\hat{\mathbf{x}}, \hat{\mathbf{y}}\hat{\mathbf{y}}$, and $\hat{\mathbf{z}}\hat{\mathbf{z}}$ into the spherical dyadics $\hat{\mathbf{r}}\hat{\mathbf{r}}, \hat{\boldsymbol{\theta}}\hat{\boldsymbol{\theta}}$, and $\hat{\boldsymbol{\varphi}}\hat{\boldsymbol{\varphi}}$ using the standard Cartesian-to-spherical transformation relations [34]. By performing this transformation, the dielectric tensor in spherical coordinates reads

$$\hat{\varepsilon} = \begin{pmatrix} \varepsilon_{rr} & -\varepsilon_{r\theta} & 0 \\ -\varepsilon_{r\theta} & \varepsilon_{\theta\theta} & 0 \\ 0 & 0 & \varepsilon_\perp \end{pmatrix}, \tag{7}$$

with $\varepsilon_\pm = (\varepsilon_{zz} \pm \varepsilon_{xx})/2$ and $\varepsilon_\perp = \varepsilon_{xx}$. We have then defined $\varepsilon_{rr} = \varepsilon_+ + \varepsilon_- \cos(2\theta)$, $\varepsilon_{\theta\theta} = \varepsilon_+ - \varepsilon_- \cos(2\theta)$ and $\varepsilon_{r\theta} = \varepsilon_- \sin(2\theta)$. The fact that the tensor components depend on the polar coordinate θ makes the problem to find the eigenmodes of the spherical resonator much more difficult. Moreover, in an anisotropic system it is in general no longer possible to divide the electric and magnetic fields in their TM and TE components. In order to overcome the latter problem, we will focus our attention on the case of small anisotropy, i.e., $\lambda = \varepsilon_-/\varepsilon_+ \ll 1$ (this approximation is very good if we consider, for example, a dielectric sphere made of lithium niobate (LiNbO$_3$) for which we have $\varepsilon_{xx} = 5.3$, $\varepsilon_{zz} = 6.47$, and therefore $\lambda \simeq 0.01$). In such a way the fields can be decomposed in quasi-TE and quasi-TM oscillations, allowing us to solve the problem using the method of Debye potentials. To this aim, and for the sake of clarity, let us rewrite the set of Eqs. (1) for the anisotropic case as follows:

$$\frac{\partial}{\partial r}(r\sin\theta E_\varphi) - \frac{\partial}{\partial\varphi}(E_r) = ik_0\sin\theta(rH_\theta), \tag{8a}$$

$$\frac{\partial}{\partial\theta}(E_r) - \frac{\partial}{\partial r}(rE_\theta) = ik_0(rH_\varphi), \tag{8b}$$

$$\frac{\partial}{\partial\varphi}(rE_\theta) - \frac{\partial}{\partial\theta}(r\sin\theta E_\varphi) = ik_0 r\sin\theta(rH_r), \tag{8c}$$

and

$$\frac{\partial}{\partial r}(r\sin\theta H_\varphi) - \frac{\partial}{\partial\varphi}(H_r)$$
$$= ik_0\sin\theta[\varepsilon_{r\theta}(rE_r) - \varepsilon_{\theta\theta}(rE_\theta)], \tag{9a}$$

$$\frac{\partial}{\partial\theta}(H_r) - \frac{\partial}{\partial r}(rH_\theta) = -ik_0\varepsilon_\perp(rE_\varphi), \tag{9b}$$

$$\frac{\partial}{\partial\varphi}(rH_\theta) - \frac{\partial}{\partial\theta}(\sin\theta rH_\varphi)$$
$$= -ik_0 r\sin\theta[\varepsilon_{rr}(rE_r) + \varepsilon_{r\theta}(rE_\theta)]. \tag{9c}$$

As in the previous section, we solve the problem for the quasi-TM component of the field (i.e., $H_r = 0$); the quasi-TE solution is again obtained using similar arguments.

These equations can be rewritten using the quasi-TM and quasi-TE potentials (U and V respectively), as follows (see Appendix A for detailed calculations):

$$\hat{L}_H V = 2i\varepsilon_- k_0\hat{\Upsilon}\frac{\partial U}{\partial\varphi}, \tag{10a}$$

$$\hat{L}_E U = 2i\varepsilon_- k_0\hat{\Upsilon}\frac{\partial V}{\partial\varphi}, \tag{10b}$$

where we have defined

$$\hat{L}_H = (\nabla_\perp^2 + r^2\hat{l}_x)\hat{l}_\theta - 2\varepsilon_- k_0^2\frac{\partial^2}{\partial\varphi^2},$$

$$\hat{L}_E = \hat{\Xi}_0 + \lambda\hat{\Xi}\hat{l}_x,$$

$$\nabla_\perp^2 = \frac{1}{\sin\theta}\frac{\partial}{\partial\theta}\sin\theta\frac{\partial}{\partial\theta} + \frac{1}{\sin^2\theta}\frac{\partial^2}{\partial\varphi^2},$$

$$\hat{\Upsilon} = \left(r\hat{l}_x - 2\frac{\partial}{\partial r}\right)\cos\theta - \sin\theta\frac{\partial^2}{\partial\theta\partial r},$$

$$\hat{\Xi}_0 = \left[\nabla_\perp^2 + r^2\frac{\partial^2}{\partial r^2} + \varepsilon_+(1 - \lambda^2)k_0^2 r^2\right]\hat{l}_x$$
$$+ 2\varepsilon_-(1 - \lambda)k_0^2\frac{\partial^2}{\partial\varphi^2},$$

$$\hat{\Xi} = \cos(2\theta)\left[r^2\frac{\partial^2}{\partial r^2} - \nabla_\perp^2 + 3\left(1 - r\frac{\partial}{\partial r}\right)\right]$$
$$+ \left(3 - 2r\frac{\partial}{\partial r}\right)\sin(2\theta)\frac{\partial}{\partial\theta}$$
$$+ \left(1 - r\frac{\partial}{\partial r}\right) - 2\frac{\partial^2}{\partial\varphi^2}, \tag{11}$$

and $\lambda = \varepsilon_-/\varepsilon_+$ is the anisotropy parameter.

From Eqs. (10) it is evident that the anisotropy gives rise to a coupling between the two quasipotentials U and V; this coupling is absent in the isotropic case in which the two potentials are independent of each other. These equations, in fact, contain the isotropic solution in the limit of $\lambda = 0$. Making this substitution in Eq. (10b) and using the definition of the operator $\hat{L}_H$, we obtain

$$(\nabla_\perp^2 + r^2\hat{l}_x)\hat{l}_\theta U = 0. \tag{12}$$

Because we set $\lambda = 0$, the two differential operators $\hat{l}_x$ and $\hat{l}_\theta$ (whose explicit form is given in Appendix A) are equal, since $\varepsilon_{\theta\theta} = \varepsilon_+ - \varepsilon_- \cos 2\theta = \varepsilon_+ = \varepsilon$ and $\varepsilon_\perp = \varepsilon$, i.e., no anisotropy is present anymore. We now define $\hat{l}_\theta U = A$ as the isotropic potential, and we assume that this potential can

be written in a separable way, i.e., $A(r,\theta,\varphi) = \Psi(r)Y_{nm}(\theta,\varphi)$, where $Y_{nm}(\theta,\varphi)$ are the eigensolutions of the angular momentum operator, whose eigenvalues are $-n(n+1)$ [i.e., $\nabla_\perp^2 Y_{nm} = -n(n+1)Y_{nm}$]. Substitution of this ansatz into the previous equation and consequent simplification of the angular part then gives the following radial equation:

$$[n(n+1) - r^2\hat{l}_x]\Psi(r) = 0, \qquad (13)$$

that is precisely the radial equation for the isotropic potential. The same procedure applied to the quasipotential V gives its isotropic counterpart.

Since we stated that the anisotropy is small (i.e., $\lambda \ll 1$), then we can use the method of separations of variable to solve the coupled equations (10). We then write the quasipotentials as follows:

$$U(r,\theta,\varphi) = \sum_{n,m,q} u_{q,n}(r)Y_{nm}(\theta,\varphi), \qquad (14a)$$

$$V(r,\theta,\varphi) = \sum_{n,m,q} v_{q,n}(r)Y_{nm}(\theta,\varphi), \qquad (14b)$$

where we note that, in general, the radial component of the eigenmode can depend both on the radial (q) and polar (n) indexes. This is very easy to justify in the isotropic case, where the index of the radial Bessel function is a function of the polar index, i.e., $\nu = n + 1/2$, as can be seen in any textbook [34]. It is then straightforward to generalize this behavior even to the anisotropic case.

The polar index n determines the number of field nodes along the polar coordinate θ, the azimuthal number m characterizes the nodes in the φ direction, and, finally, the radial index q gives the number of field oscillations along the radial direction r that is related with the solution of the characteristic equation. Substituting Eq. (14) into Eq. (10), using relationships (4) and (5) of Ref. [35], and equating the terms with equal angular part $Y_{nm}(\theta,\varphi)$ we obtain the following set of differential equations for the radial components $u_p(r)$ and $v_p(r)$ of the quasipotentials [36]:

$$a_{1,n}^{TM}u_n - a_{2,n-2}^{TM}u_{n-2} - a_{3,n+2}^{TM}u_{n+2}$$
$$= -2\varepsilon_-mk_0[b_{1,n-1}v_{n-1} - b_{2,n+1}v_{n+1}], \qquad (15a)$$
$$a_{1,n}^{TE}v_n - \lambda\left(a_{2,n-2}^{TE}v_{n-2} + a_{3,n+2}^{TE}v_{n+2}\right)$$
$$= -2\lambda mk_0[b_{1,n-1}u_{n-1} - b_{2,n+1}u_{n+1}]. \qquad (15b)$$

For the sake of clarity, the expressions of the operators $a_i^{TM/TE}$ and b_i are reported in Appendix B.

These equations require, in general, a numerical approach to be solved. However, in the limit of small anisotropy, i.e., $\lambda \ll 1$, a solution to Eqs. (15) can be searched in terms of power series in the factor λ. The zeroth-order solution gives the solution of the isotropic spherical resonator in terms of the Riccati-Bessel functions [see Eq. (13)]. The first-order solution, i.e., the anisotropic correction we are searching for, is obtained by neglecting the terms that are proportional to λ^2 in Eqs. (15): however, the resulting equations contain in the right-hand side a term that is not zero (like in the zeroth-order solution) but depends on the quasipotentials $u_{n\pm1}$ and $v_{n\pm1}$. This coupling among neighbor radial modes is a signature of the anisotropy, that on one hand breaks the azimuthal degeneracy [the azimuthal quantum number appears in the

definition of the coefficients of Eqs. (15)] and on the other hand results in a coupling between radial modes. Although this coupling results in an impossibility of an analytic solution, it can be demonstrated [35] that these terms are of the order λ^2 and at the first order they can be neglected. With this argument, Eqs. (15) at the leading order λ read

$$\left[r^2\left(\frac{d^2}{dr^2} + \frac{\gamma_1^2}{r^2}\right) - n(n+1)\right]l_+u_n(r) = 0, \qquad (16a)$$

$$\left[r^2\left(\frac{d^2}{dr^2} + \frac{\gamma_2^2}{r^2}\right) - n(n+1)\right]l_+v_n(r) = 0, \qquad (16b)$$

where γ_1 and γ_2 are the TM and TE (respectively) anisotropic factor given by

$$\gamma_1^2 = k_0^2\varepsilon_+\left\{1 - \lambda\left[1 - \frac{2m^2}{n(n+1)}\right]\right\}, \qquad (17a)$$

$$\gamma_2^2 = k_0^2\varepsilon_+\left\{1 - \lambda\left[\frac{1-4m^2}{4n(n+1)-3} + \frac{2m^2}{n(n+1)}\right]\right\}. \qquad (17b)$$

Equations (16) have the same structure of the radial equation for the isotropic case [34]. The only difference is the presence of the γ_i terms that modify the arguments of the Riccati-Bessel functions and the quasipotentials can be written as

$$U_{nm}(r,\theta,\varphi) = C_{int/ext}z_\nu(x)Y_{nm}(\theta,\varphi), \qquad (18a)$$

$$V_{nm}(r,\theta,\varphi) = C_{int/ext}z_\nu(x)Y_{nm}(\theta,\varphi), \qquad (18b)$$

where $z_\nu(x)$ corresponds to $j_\nu(x)$ inside the sphere and to $h_\nu^{(1)}(x)$ outside the sphere. Note also that inside the sphere, where the anisotropy exists, $x = \gamma_i r$, while outside the sphere $x = k_0 r$ (the surrounding medium is still isotropic). Substituting these expressions in Eqs. (A4) in Appendix A, we obtain all the components of the electric and magnetic fields in a uniaxial anisotropic spherical resonator,

$$E_r = \frac{n(n+1)}{r^2}\left[\sqrt{\frac{\pi}{2}}z_\nu(\gamma_1 x)Y_{n,m}(\theta,\varphi)\right], \qquad (19a)$$

$$rE_\theta = -\frac{\partial^2}{\partial r\partial\theta}\left[\sqrt{\frac{\pi}{2}}z_\nu(\gamma_1 x)Y_{n,m}(\theta,\varphi)\right], \qquad (19b)$$

$$rE_\varphi = \frac{1}{\sin\theta}\frac{\partial^2}{\partial r\partial\varphi}\left[\sqrt{\frac{\pi}{2}}z_\nu(\gamma_1 x)Y_{n,m}(\theta,\varphi)\right], \qquad (19c)$$

$$H_r = 0 \qquad (19d)$$

$$rH_\theta = -\frac{ik_0\varepsilon_\perp}{\sin\theta}\frac{\partial}{\partial\varphi}\left[\sqrt{\frac{\pi}{2}}z_\nu(\gamma_1 x)Y_{n,m}(\theta,\varphi)\right], \qquad (19e)$$

$$rH_\varphi = ik_0\varepsilon_\perp\frac{\partial}{\partial\theta}\left[\sqrt{\frac{\pi}{2}}z_\nu(\gamma_1 x)Y_{n,m}(\theta,\varphi)\right], \qquad (19f)$$

for quasi-TM fields. Similar expressions can be written for the quasi-TE fields by replacing γ_1 with γ_2, exchanging the role of the electric and magnetic field and setting $\varepsilon_\perp = 1$.

The characteristic equation can be found by applying the boundary conditions and it turns out to be ($\tilde{\gamma}_i = \gamma_i/k_0\sqrt{\varepsilon_+}$)

$$\tilde{\gamma}_1\frac{[j_\nu(\gamma_1 kR)]'}{j_\nu(\gamma_1 kR)} = \frac{\varepsilon_\perp}{\sqrt{\varepsilon_+}}\frac{\left[h_\nu^{(1)}(k_0 R)\right]'}{h_\nu^{(1)}(k_0 R)} \qquad (20)$$

for the quasi-TM waves. The characteristic equation for quasi-TE waves is obtained by replacing $\tilde{\gamma}_1$ with $\tilde{\gamma}_2$, γ_1 with γ_2, and $\varepsilon_\perp$ with 1.

As can be seen from the previous equations, in the small anisotropy regime, the only effect of the anisotropy is a rescaling of the radial coordinate; this is in accordance with the fact that a uniaxial crystal shows two different refractive indexes: one in plane ($\sqrt{\varepsilon_{xx}}$) and the other out of plane ($\sqrt{\varepsilon_{zz}}$). Different refractive indexes correspond to different optical paths, and this is exactly reflected in the rescaling effect of the anisotropy onto the radial part of the modes of the resonator. Note also that at this level of analysis, the anisotropy does not affect the angular structure (θ and φ) of the modes. Another difference with respect to the isotropic case is the value of the coefficients on the right-hand side of the characteristic equations: while the coefficient for the quasi-TE wave is analogous to its isotropic counterpart (if we substitute the isotropic dielectric constant ε with the anisotropy-averaged dielectric constant ε_+), the coefficient for the quasi-TM wave reveals the presence of the anisotropy, since it is a ratio between the in-plane dielectric constant and the anisotropy-averaged one. This is not so surprising because for a dielectric uniaxial crystal, only the TM component suffers direct anisotropy, while the TE component does not, because the crystal is magnetically isotropic.

IV. WHISPERING GALLERY MODES

A. Radial functions with large indices

The term whispering gallery mode (WGM) commonly addresses the set of modes with a large index n; strictly speaking, the real WGMs are only those for which it results that $n = m$ and the radial wave function shows no roots inside the resonator. However, modes with indices $n \neq m$ and with $q > 1$, but close to unity, have properties that are close to those of WGMs: this means that there is no great difference between a "pure" WGM and other modes with nearest indices.

To study such modes, the first thing we have to do is to find a suitable approximation of Riccati-Bessel functions for large index. This approximation is useful either from the numerical (where computing Bessel functions of a large index is highly time consuming) or analytical (where the approximation gives the possibility to work with easier functions that better suit the problem) point of view. The appropriate approximation, however, should be searched bearing in mind that the argument of the Bessel function for a WGM near the sphere surface is of the order of its index, i.e., $\nu/x \simeq 1$. By introducing the following change of variables:

$$\zeta = \left(\frac{2}{\nu}\right)^{1/3}(\nu - x),$$

the Bessel function inside the dielectric resonator can be very well approximated by the Airy function of the first kind Ai as follows [37]:

$$j_\nu(x) \simeq \sqrt{2}\left(\frac{\nu}{2}\right)^{1/6}\text{Ai}(\zeta), \tag{21a}$$

$$\frac{d}{dx}[j_\nu(x)] \simeq -\sqrt{2}\left(\frac{2}{\nu}\right)^{1/6}\frac{d}{d\zeta}[\text{Ai}(\zeta)]. \tag{21b}$$

The accuracy of this approximation is of the order ν^{-1}; if ν exceeds 1000, this accuracy is very satisfactory for many
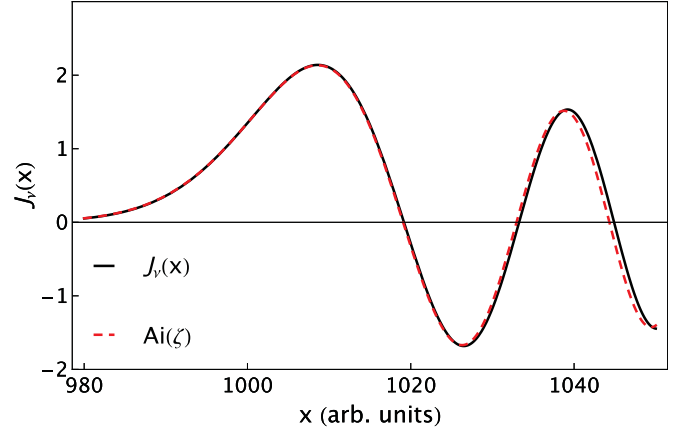
FIG. 3. (Color online) Comparison between $j_\nu(x)$ (solid black line) and its Airy approximation from Eq. (21a) (dashed red line) for $\nu = 1000.5$. The approximation holds very well up to $x \simeq \nu$, while for x larger than ν (say for $x > 1020$) it starts to fail.

calculations. This can be seen in Fig. 3, where Bessel functions of high order are compared with their Airy approximation and in Fig. 4, where it is shown that as ν grows, the accuracy of the approximation became more satisfactory.

For the solution outside the resonator (the Hankel function of the first kind) various approximations are available. Here we use the following [38]:

$$h_\nu^{(1)}(x) \equiv f(\eta) = \simeq \frac{e^{i[\nu(\tan\eta - \eta) - \pi/4]}}{\sqrt{\frac{\pi}{2}\tan\eta}}$$

$$\times \left\{1 - \frac{i}{\nu}\left(\frac{1}{8\tan\eta} + \frac{5}{24}\frac{1}{\tan^3\eta}\right) + O[\nu^{-2}]\right\} \tag{22}$$

where $\cos\eta = \nu/x$; if ν is large enough (heuristically $\nu > 1000$) the imaginary term inside the curly braces can be neglected. The choice of this approximation rather than the one presented in Ref. [30] resides in the fact that while the
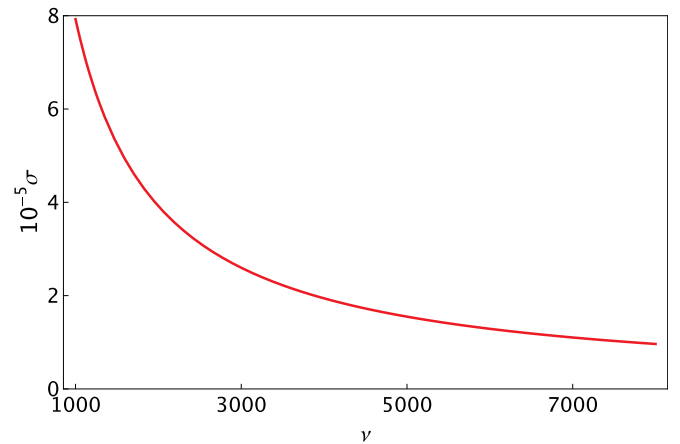
FIG. 4. (Color online) The figure shows the accuracy σ as a function of the Bessel index ν; the accuracy is defined as the ratio between the difference of the true function $j_\nu(\nu)$ and its Airy approximation Ai(ζ) and their sum, i.e., $\sigma = [j_\nu(\nu) - \text{Ai}(\zeta^*)]/[j_\nu(\nu) + \text{Ai}(\zeta^*)]$, where ζ^* is ζ evaluated for $x = \nu$. As can be seen, as ν grows, the approximation becomes more precise.
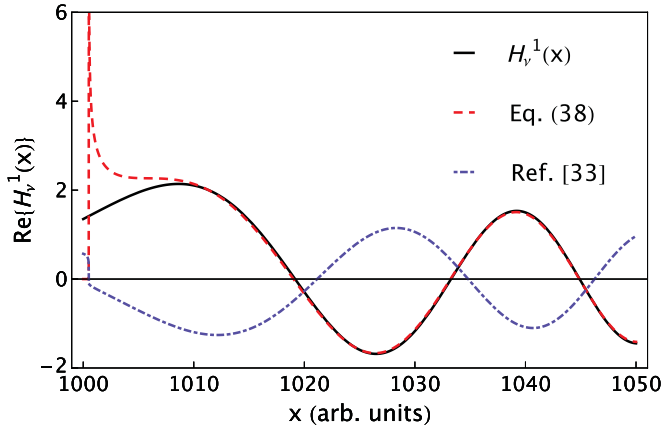
FIG. 5. (Color online) Comparison between the real part of $h_\nu^{(1)}(x)$ (black solid line), Eq. (22) (red dashed line) and Eq. (31) of Ref. [30] (blue dot-dashed line) for $\nu = 1000.5$. Our approximation works very well in the region in which the argument is greater than the index (i.e., $x > 1010$), while the approximation presented in Ref. [30] is out of phase with respect to the Hankel function.

former is very good when the argument of the Hankel function is greater than the index (that is precisely the case of the outer functions), the latter is not suitable in this region, either for being out of phase with respect to the Hankel function (as shown in Figs. 5 and 6) or to not approximate in the correct way the original function (Fig. 7). Moreover, Fig. 7 shows that the field outside the resonator has all the characteristics of an evanescent wave, i.e., it decays exponentially as the distance from the resonator surface grows.

In order to justify this evanescent behavior outside the resonator, one can directly solve the equation for the radial part of the field in the limit $r > R$ (but still close to the resonator surface), where the terms $x = k_0 r$ outside the derivation symbol can be substituted with $k_0 R$, leading to the following equation:

$$\frac{d^2 Z}{dx^2} + \frac{1}{k_0 R}\frac{dZ}{dx} + \left[1 - \frac{\nu^2}{(k_0 R)^2}\right]Z = 0, \qquad (23)$$

whose solution is

$$Z_\nu(x) = C_0 e^{-\delta x}, \qquad (24)$$
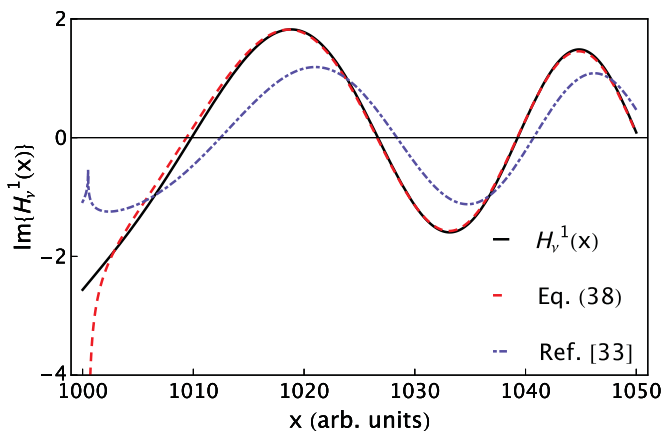
FIG. 6. (Color online) Same as Fig. 5 but the comparison is made for the imaginary part.
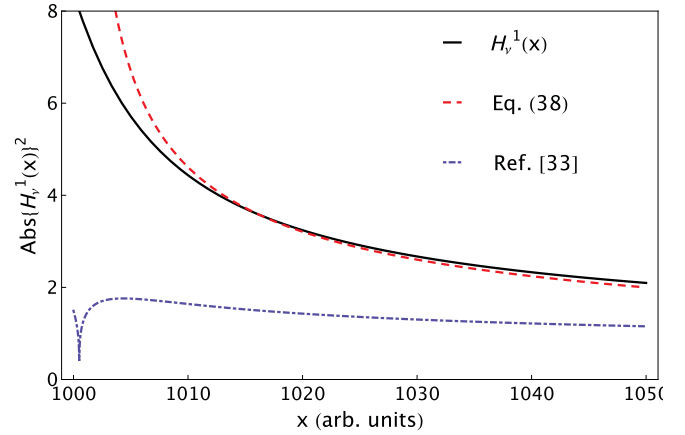
FIG. 7. (Color online) Same as Fig. 5 but the comparison is made for the absolute value; note in this case how the approximation presented in Ref. [30] completely fails to approximate the Hankel function.

where

$$\delta = \left[\sqrt{\left(\frac{\nu}{k_0 R}\right)^2 - 1 + \frac{1}{4(k_0 R)^2}} - \frac{1}{2k_0 R}\right].$$

This is, as expected, the expression of an exponentially decreasing field that is in perfect agreement with the hypothesis that the field outside the resonator is evanescent due to total internal reflection.

It can be, moreover, noted that the oscillatory behavior of the field components outside the resonator (as depicted in Figs. 5 and 6 for the radial component of the electric field) is not in contrast with this hypothesis, since it only represents the behavior of the Hankel function as $r \to \infty$, i.e., it behaves like a runaway wave whose intensity is decreasing as $1/r^2$. In the case of WGMs, however, no radiation will run away toward infinity since the external field is evanescent, i.e., the radiation is trapped inside the WGM and rapidly decreases toward zero when the field goes outside the resonator.

B. Angular functions with large indices

For large indices n, the WGM field is concentrated in a narrow interval of angles θ near $\theta_0 = \pi/2$; this makes it possible to approximate the associated Legendre functions (i.e., the θ part of the scalar spherical harmonics) with large indices, with Hermite polynomials with small indices, as follows:

$$Y_{nm}(\theta,\varphi) \simeq \frac{\sqrt{m}}{2^w \sqrt{\pi}\, w!} H_w(\sqrt{m}\alpha) e^{-(m/2)\alpha^2} e^{im\varphi}. \qquad (25)$$

Detailed calculations for obtaining this result are shown in Appendix C.

C. Roots of characteristic equations

The approximations exploited in the previous section are very useful in finding an analytical solution to the characteristic equation for the eigenfrequencies of the resonator; however, due to the anisotropy, some changes in the definition of the variables used above must be done. First of all, the x appearing in Eqs. (21) and (22) has to be different for the inner and outer

functions, due to the fact that the anisotropy is confined only inside the resonator; we can then define $x = k_0 R$ as the outer variable and by consequence the inner variable results to be $y = \tilde{\gamma}_i \sqrt{\varepsilon_+} x$. Then, the definition of ζ must be changed into $\zeta = (2/\nu)^{1/3} (\nu - y)$. After that, by substituting Eqs. (21) and (22) into Eq. (20), the characteristic equation for the quasi-TM field gives [39]

$$
\tilde{\gamma}_1 \frac{1}{\mathrm{Ai}(\zeta)} \frac{d\,\mathrm{Ai}(\zeta)}{d\zeta} = \frac{\varepsilon_\perp}{\sqrt{\varepsilon_+}} \left(\frac{\nu}{2}\right)^{1/3}
$$
$$
\times \left[\frac{1}{4}\left(\frac{2x}{x^2 - \nu^2}\right) - i\sqrt{1 - \frac{\nu^2}{x^2}}\right], \quad (26)
$$

the equation for the quasi-TE field can be deduced by this one upon changing $\tilde{\gamma}_1$ with $\tilde{\gamma}_2$ and putting $\varepsilon_\perp = 1$.

In order to find an approximate formula for the solutions of this equation, let us first analyze the limiting case in which $\nu \to \infty$; in this case the right-hand side of the equation goes to infinity and the only possible solution is that $\mathrm{Ai}(\zeta) = 0$, whose solutions are the zeros of the Airy function ζ_q. Let us denote with $\Delta\zeta_q$ the first-order correction to these roots; expanding both the left-hand and right-hand sides of Eq. (26) in power series with a first-order accuracy to terms $\Delta\zeta_q$ we can obtain the first-order correction to the roots ζ_q, whose expression is

$$
\Delta\zeta_q = \frac{\tilde{\gamma}_1 \sqrt{\varepsilon_+}}{\varepsilon_\perp \alpha} \left(\frac{2}{\nu}\right)^{1/3}, \quad (27)
$$

where

$$
\alpha = \frac{x_q}{2(x_q^2 - \nu^2)} - i\sqrt{1 - \frac{\nu^2}{x_q^2}}, \quad (28)
$$

and x_q is obtained by substituting the value of the first zero of the Airy function ($\zeta_q = -2.338\,11$) into the definition of ζ and inverting that relation with respect to x.

Taking into account the definition of ζ, the eigenvalues of the wave numbers for the anisotropic resonator can be represented in the following explicit form:

$$
k_{0q} = \frac{\nu - \left(\frac{2}{\nu}\right)^{1/3}(\zeta_q + \Delta\zeta_q)}{\tilde{\gamma}_1 \sqrt{\varepsilon_+} R}. \quad (29)
$$

Note that because the quantity $\Delta\zeta_q$ is complex, the wave number is also complex. The real part of the wave number then determines the eigenfrequencies of the mode. Complex eigenfrequencies are fully compatible with the open cavity. As can be seen from Eq. (27), this approximation has an accuracy of $\nu^{-1/3}$. More accurate asymptotic expressions that allow the calculation of the positions of resonances of the modes in an isotropic dielectric spherical resonator have been largely studied in literature (see, for example, Refs. [40–45] and references therein) and they were given with various accuracy with respect to the index ν; in Ref. [45] analytic calculations are carried out to the order $\nu^{-1/3}$, in Ref. [41] the eigenfrequencies are calculated with an accuracy of $O[\nu^{-2/3}]$, while in Ref. [44] the authors give an expression up to the order $O[\nu^{-8/3}]$. Here we report the anisotropic correction of the formula found in
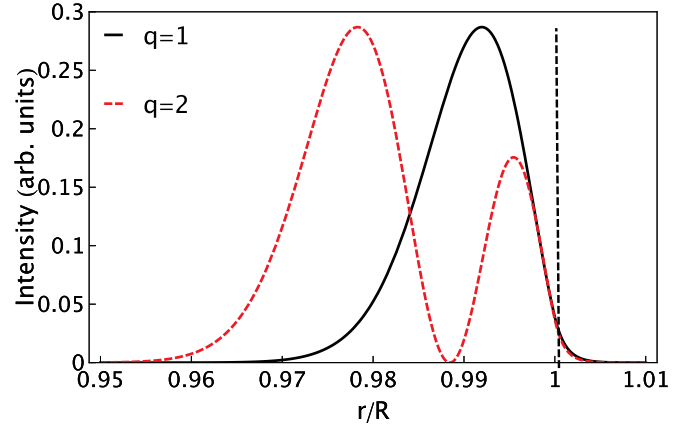
FIG. 8. (Color online) Radial part of the fundamental (black solid line) and first excited (red dashed line) WGM for the anisotropic resonator; the vertical dashed line indicates the position of the resonator surface. The fundamental mode has indices $n = m = 1000$ and $q = 1$, while the first excited mode has the same n and m indices, but $q = 2$.

Ref. [40] that gives the eigenfrequencies with a precision of the order of $O[\nu^{-1}]$,

$$
\tilde{\gamma}_i x_\nu^{(q)} = \left\{ \nu - \left(\frac{\nu}{2}\right)^{1/3} \zeta_q - \sqrt{\frac{\varepsilon_+}{\varepsilon_+ - 1}} P \right.
$$
$$
+ \frac{3}{10}\left(\frac{1}{4\nu}\right)^{1/3} \zeta_q^2 - \left(\frac{1}{2\nu^2}\right)^{1/3} \left(\frac{\varepsilon_+}{\varepsilon_+ - 1}\right)^{3/2}
$$
$$
\left. \times P\left(\frac{2}{3} P^2 - 1\right) \zeta_q + O[\nu^{-1}] \right\}, \quad (30)
$$

where $P = 1/(\tilde{\gamma}_1 \varepsilon_+)$ for quasi-TM modes and $P = \varepsilon_\perp/(\tilde{\gamma}_2 \varepsilon_+)$ for quasi-TE modes.

D. Whispering gallery modes

We now have all the elements for writing the explicit expressions for the radial, polar, and azimuthal components of the quasi-TM and quasi-TE WGMs. Taking approximations (21), (22), and (25) and substituting them in Eqs. (19) give us the explicit expressions of the quasi-TM whispering gallery modes of a spherical anisotropic resonator. Similar expressions can be written even for the quasi-TE WGMs.

We now concentrate our attention on the behavior of these modes. Figures 8 and 9 show the behavior of the fundamental quasi-TM radial (no nodes in radial direction, i.e., $q = 1$) and polar (i.e., $n = m$) WGM component $r^2 E_r$ and the "first excited" radial ($q = 2$) and polar ($m = n + 1$) mode for the same component of the quasi-TM field; the physical parameters have been set to be $\varepsilon_{xx} = 5.30$, $\varepsilon_{zz} = 6.47$ (LiNbO₃), and $\lambda = 1064$ nm. Note that the radial component has its maximum very close to the sphere surface (dashed vertical line in Fig. 8), and its position shifts on the left, i.e., on the inner part of the resonator as the radial number q increases. The polar part, instead, is localized around $\theta = \pi/2$ in its fundamental state and, as m becomes smaller than n, the maxima of the polar component tent to repel each other from $\theta = \pi/2$.
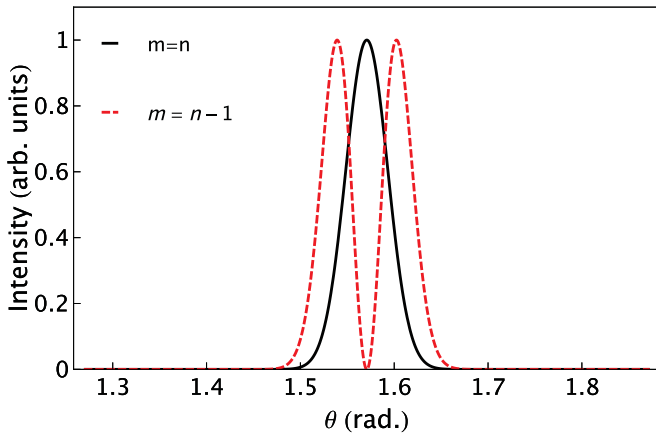
FIG. 9. (Color online) Polar part of the fundamental (black solid line) and first polar-excited (red dashed line) WGM for the anisotropic resonator. The fundamental mode has indices $n = m = 1000$ and $q = 1$, while the first polar-excited mode has $n = 1000$, $m = n - 1$, and $q = 1$.

In Figs. 10–13 the intensity distribution of the *total* electric field of a quasi-TM (i.e., $\mathbf{E}_{TM} = E_r \hat{r} + E_\theta \hat{\theta} + E_\varphi \hat{\varphi}$) is shown; $\hat{r}, \hat{\theta}$ and $\hat{\varphi}$ represent the unit vectors of the spherical basis (r, θ, φ). In order to obtain the intensity distribution of such a field, one has to sum the square modulus of each component of the electric field; however, in this particular case, the contribution of E_θ and E_φ is very small and localized at the resonator surface, and the total field is, with a good level of approximation, fully determined by its radial component. The intensity distribution for the magnetic-field components of a quasi-TM mode can be straightforwardly obtained by noting that the H_θ component of the magnetic field has the same intensity distribution as the radial electric-field component E_r and the H_φ component, because of the presence of the
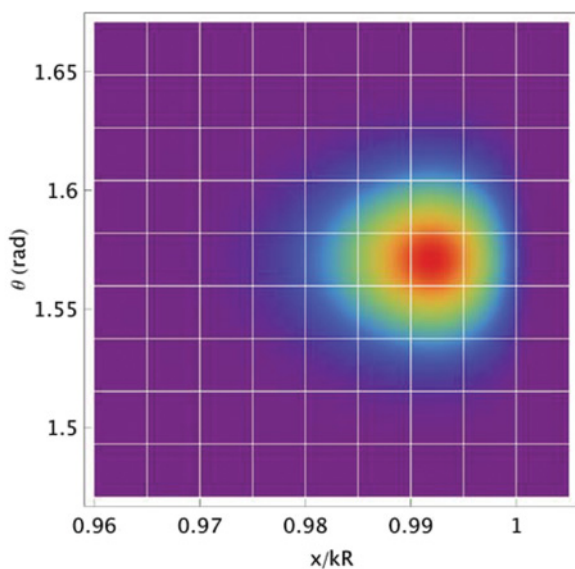
FIG. 10. (Color online) Intensity distribution of the electric field of the fundamental quasi-TM WGM. The WGM quantum numbers are $n = m = 1000$, $q = 1$.
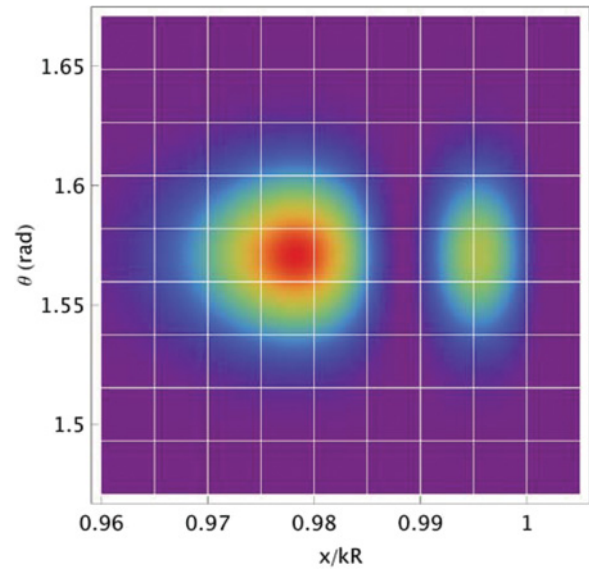
FIG. 11. (Color online) Same as Fig. 10 but for $q = 2$; this mode represents the first radially excited WGM.

derivative with respect to θ, has the same intensity distribution as the one depicted in Fig. 12.

As the reader can see from these figures, the field is nonzero even after the resonator surface ($x = 1$); this is not surprising because in this region the total field is evanescent due to the fact that it has been total internal reflected by the resonator, i.e., the field is confined in the resonator WGM.

V. CONCLUSIONS

In this work, we have developed a classical-optics theory for a uniaxial spherical whispering gallery resonator. We have presented and discussed the mode structure in the limit of small anisotropy for such a resonator, and obtained its spectrum. Moreover, we have furnished a thorough discussion
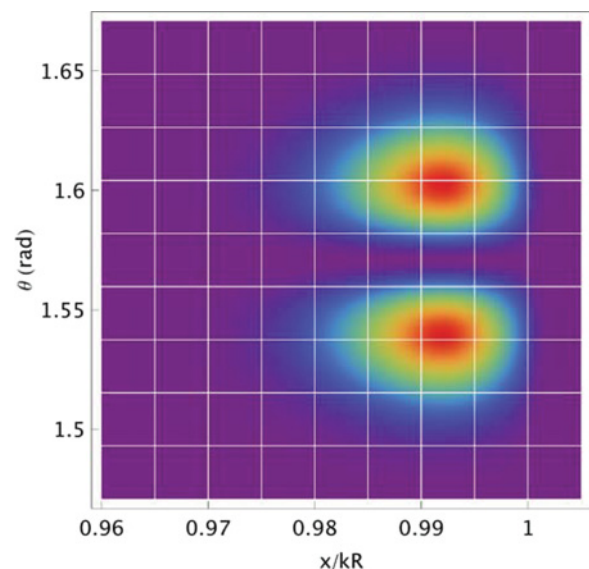
FIG. 12. (Color online) Same as Fig. 10 but for $n - m = 1$; this mode represents the first polar excited WGM.
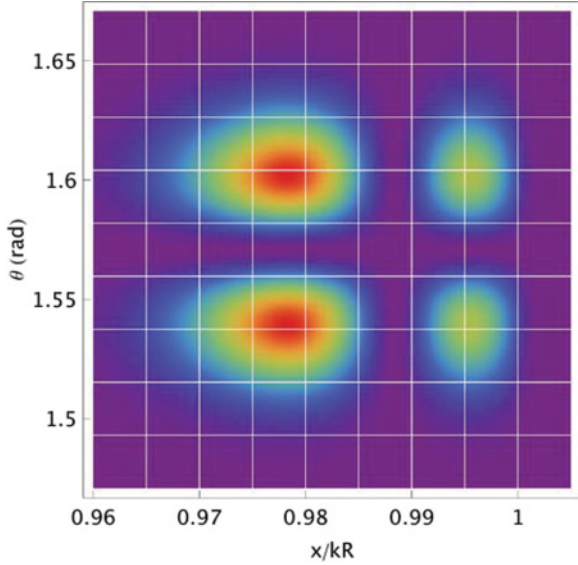
FIG. 13. (Color online) Same as Fig. 10 but for $n - m = 1$ and $q = 2$; this mode represents the first radially and polar excited WGM.

on the boundary conditions and asymptotic expressions for the electromagnetic field in WGRs. Our results may be easily generalized to achieve a quantum theory of WGRs.

APPENDIX A: DERIVATION OF EQS. (10)

In order to obtain from the set of Maxwell's equations in the anisotropic case (8) and (9), we follow the solving procedure described in Ref. [35]. Let us combine Eq. (9b) and the derivative with respect to r of Eq. (8a) and introduce the W setting $H_r = 0$ and letting W be the function that realized the equality between the φ and θ components of the electric field in Eq. (8c). We will obtain

$$
\begin{cases}
\frac{\partial}{\partial r}(r H_\theta) = \frac{1}{\sin\theta} i k_0 \varepsilon_\perp \frac{\partial W}{\partial \varphi}, \\
\frac{\partial^3}{\partial r^2 \partial \varphi}(W) - \frac{\partial^2}{\partial r \partial \varphi}(E_r) = i k_0 \sin\theta \frac{\partial}{\partial r}(r H_\theta).
\end{cases}
$$

If we substitute the expression of $\frac{\partial}{\partial r}(r H_\theta)$ obtained from the first equation into the second one and if we define the differential operator $\hat{l}_x = \partial^2/\partial r^2 + k_0^2 \varepsilon_\perp$ we obtain

$$
\frac{\partial E_r}{\partial r} = \hat{l}_x W. \tag{A1}
$$

Combining now Eq. (9a), and the derivative with respect to r of Eq. (8b) gives

$$
\begin{cases}
\frac{\partial}{\partial r}(r \sin\theta H_\varphi) = i k_0 r \sin\theta \left(\varepsilon_{r\theta} E_r - \frac{1}{r} \varepsilon_{\theta\theta} \frac{\partial W}{\partial \theta} \right), \\
\frac{\partial^2}{\partial r \partial \theta}(E_r) - \frac{\partial^2}{\partial r^2}(r E_\theta) = i k_0 \frac{\partial}{\partial r}(r H_\varphi).
\end{cases}
$$

Again, by substituting the expression for $\frac{\partial}{\partial r}(r H_\varphi)$ obtained from the first equation into the second one, and by defining the differential operator $\hat{l}_\theta = \partial^2/\partial r^2 + k_0^2 \varepsilon_{\theta\theta}$ we obtain

$$
\left[k_0^2 \varepsilon_{r\theta} r + \frac{\partial^2}{\partial r \partial \theta} \right] E_r = \hat{l}_\theta \frac{\partial W}{\partial \theta}. \tag{A2}
$$

By now defining W as a function of the quasi-TM potential U, let us compare Eqs. (A1) and (A2). By noting that the differential operator $\hat{l}_\theta$ commutes with the operator $(k_0^2 \varepsilon_{r\theta} r + \partial^2/\partial r \partial \theta)$ that appears in Eq. (A2), is it possible to define, after some simple algebra, the function W as a function of the quasi-TM potential U as follows:

$$
W = \frac{\partial}{\partial r}(\hat{l}_\theta U). \tag{A3}
$$

This allow us to write the components of the TM electric and magnetic field in terms of the quasi-TM potential U as follows:

$$
E_r^{TM} = \hat{l}_x \hat{l}_\theta U, \tag{A4a}
$$

$$
r E_\varphi^{TM} = \frac{1}{\sin\theta} \frac{\partial^2}{\partial r \partial \varphi}(\hat{l}_\theta U), \tag{A4b}
$$

$$
r E_\theta^{TM} = \left(\varepsilon_{r\theta} k_o^2 r + \frac{\partial^2}{\partial r \partial \theta} \right) \hat{l}_x U, \tag{A4c}
$$

$$
H_r^{TM} = 0, \tag{A4d}
$$

$$
r H_\theta^{TM} = \frac{i k_0 \varepsilon_\perp}{\sin\theta} \frac{\partial}{\partial \varphi}(\hat{l}_\theta U), \tag{A4e}
$$

$$
r H_\varphi^{TM} = i k_0 \left[\varepsilon_{\theta\theta} \frac{\partial}{\partial \theta} + \varepsilon_{r\theta} \left(1 - r \frac{\partial}{\partial r} \right) \right] \hat{l}_x U. \tag{A4f}
$$

Again, similar expressions can be found for the quasi-TE fields and the quasi-TE potential V. Their explicit expressions can be found in Ref. [46].

By now considering a generic electric and magnetic field, whose components can be written as the superposition of the quasi-TE and quasi-TM oscillations, i.e., $E_i = E_i^{TM} + E_i^{TE}$ and $H_i = H_i^{TM} + H_i^{TE}$, by substituting these field expressions in Eqs. (8) and (9), after some algebra we arrive at a set of two coupled equations (10).

APPENDIX B: COEFFICIENTS OF EQS. (15)

Here are reported the explicit expressions of the coefficients that appear on Eqs. (15). In order to express them in a compact form, let us introduce the following quantities:

$$
g_\pm = k_o^2 \varepsilon_\pm,
$$

$$
f_n = \frac{1}{2n + 2},
$$

$$
T_n = r^2 \hat{l}_x - n(n + 1),
$$

$$
l_+ = \frac{\partial^2}{\partial r^2} + k_0^2 \varepsilon_+.
$$

With these parameters defined, the a and bs coefficients of Eq. (15) become

$$
a_{1,n}^{TM} = T_n \left[l_+ - \frac{1 - 4m^2}{4n(n+1) - 3} g_- \right] + 2g_- m^2,
$$

$$
a_{2,n}^{TM} = 2g_-(n - m + 1)(n - m + 2) f_n f_{n+1} T_n,
$$

$$
a_{3,n}^{TM} = 2g_-(n + m)(n + m - 1) f_n f_{n-1} T_n,
$$

$$b_{1,n} = f_n(n - m + 1)\left[r\hat{l}_x - (n+2)\frac{d}{dr}\right],$$

$$b_{2,n} = f_n(n + m)\left[r\hat{l}_x + (n-1)\frac{d}{dr}\right],$$

$$a_{1,n}^{TE} = \left\{\left[r^2\frac{d^2}{dr^2} - n(n+1)\right]\left[1 + \lambda\left(\frac{1 - 4m^2}{4n(n+1) - 3}\right)\right]\right.$$

$$\left. + (1-\lambda)g_+r^2\right\}\hat{l}_x - 2m^2g_-(1-\lambda),$$

$$a_{n,2}^{TE} = 2f_n f_{n+1}(n - m + 1)(n - m + 2)$$

$$\times \left[r^2\frac{d^2}{dr^2} - (2n+3)r\frac{d}{dr} + n(n+1)\right],$$

$$a_{n,3}^{TE} = 2f_n f_{n-1}(n + m)(n + m - 1)$$

$$\times \left[r^2\frac{d^2}{dr^2} - (2n-1)r\frac{d}{dr} + (n+1)(n-3)\right].$$

APPENDIX C: APPROXIMATION OF SCALAR SPHERICAL HARMONICS FOR LARGE INDICES

The equation for the θ part of spherical harmonics is the following:

$$\frac{1}{\sin\theta}\frac{d}{d\theta}\left(\sin\theta\frac{df}{d\theta}\right) + \left[n(n+1) - \frac{m^2}{\sin^2\theta}\right]f = 0,$$

whose solutions are the associated Legendre functions $f(\theta) = P_n^m(\cos\theta)$. Since WGMs are located near the equator of the resonator, the correspondent functions $f(\theta)$ will be peaked

near the angle $\theta_0 = \pi/2$; in order to find an approximate expression for the polar part of the spherical harmonics, let us introduce the new variable $\alpha = \pi/2 - \theta$: substituting into the equation above gives

$$\frac{d^2}{d\alpha^2} - \tan\alpha\frac{df}{d\alpha} + \left[n(n+1) - \frac{m^2}{\cos^2\alpha}\right]f = 0.$$

We note that, since the modes are localized near the equator, $\alpha \ll 1$ and this allows us to expand in power series the trigonometric functions that appear in the previous equation, i.e., $\tan\alpha \simeq \alpha$ and $1/\cos^2\alpha \simeq 1 + \alpha^2$. Substituting in the previous equation, writing $f(\alpha) = G(\alpha)e^{\alpha^2/4}$, and performing the change of variables $\alpha = x/[(m^2 + 1/4)^{1/4}] = \xi x$ we obtain

$$\frac{d^2G}{dx^2} + \{\xi^2[n(n+1) - m^2] - x^2\}G = 0.$$

Introducing the quantity $w = n - m$ and remembering that WGMs are characterized by high values of the indices, i.e., $n, m \gg 1$, the first term that appears inside the curly braces can be simplified as $2w + 1$. With this substitution the last equation is precisely the Hermite-Gauss equation, whose solutions have the form $G(x) \simeq H_w(x)e^{-x^2/2}$. Function $f(\alpha)$ then becomes

$$f(\alpha) = P_n^m(\cos\theta) \simeq NH_w(\sqrt{m}\alpha)e^{-(m/2)\alpha^2},$$

where N is a normalization factor whose expression could be found by requiring that the norm of $f(\alpha)$ integrated over the real axis is 1. This equation gives the approximated form of the associated Legendre functions for WGMs; substituting it into the definition of the scalar spherical harmonics gives exactly Eq. (25).

[1] [http://en.wikipedia.org/wiki/St_Paul's_Cathedral].
[2] Baron John William Strutt Rayleigh, *The Theory of Sound: Volume II* (Dover, New York, 1945).
[3] G. Mie, Ann. Phys. **25**, 377 (1908).
[4] P. Debye, Ann. Phys. **30**, 57 (1909).
[5] M. L. Gorodetsky *et al.*, Opt. Lett. **21**, 453 (1996).
[6] I. S. Grudinin, V. S. Ilchenko, and L. Maleki Phys. Rev. A **74**, 063806 (2006).
[7] A. A. Savchenkov, V. S. Ilchenko, A. B. Matsko, and L. Maleki, Phys. Rev. A **70**, 051804(R) (2004).
[8] V. S. Ilchenko, A. A. Savchenkov, A. B. Matsko, and L. Maleki, Phys. Rev. Lett. **92**, 043903 (2004).
[9] V. S. Ilchenko *et al.*, J. Opt. Soc. Am. B **20**, 1304 (2003).
[10] G. Kozyreff, J. L. Dominguez Juarez, and J. Martorell, Phys. Rev. A **77**, 043817 (2008).
[11] A. A. Savchenkov *et al.*, Opt. Lett. **32**, 157 (2007).
[12] A. A. Savchenkov, A. B. Matsko, D. Strelakov, M. Mohageg, V. S. Ilchenko, and L. Maleki, Phys. Rev. Lett. **93**, 243905 (2004).
[13] P. Del'Haye *et al.*, Nature (London) **450**, 1214 (2007).
[14] A. A. Savchenkov, A. B. Matsko, V. S. Ilchenko, I. Solomatine, D. Seidel, and L. Maleki, Phys. Rev. Lett. **101**, 093902 (2008).
[15] I. S. Grudinin, A. B. Matsko, and L. Maleki, Phys. Rev. Lett. **102**, 043902 (2009).
[16] D. V. Strekalov *et al.*, Opt. Lett. **34**, 713 (2009).

[17] V. S. Ilchenko, A. A. Savchenkov, A. B. Matsko, and L. Maleki, Phys. Rev. Lett. **92**, 043903 (2004).
[18] T. Carmon and K. J. Vahala, Nat. Phys. **3**, 430 (2007).
[19] J. U. Fürst, D. V. Strekalov, D. Elser, M. Lassen, U. L. Andersen, C. Marquardt, and G. Leuchs, Phys. Rev. Lett. **104**, 153901 (2010).
[20] D. W. Vernooy, A. Furusawa, N. P. Georgiades, V. S. Ilchenko, and H. J. Kimble, Phys. Rev. A **57**, R2293 (1998).
[21] J. R. Buck and H. J. Kimble, Phys. Rev. A **67**, 033806 (2003).
[22] A. B. Matsko *et al.*, IPN Prog. Rep. **42**, 162 (2005).
[23] G. W. Ford and S. A. Werner, Phys. Rev. B **18**, 6752 (1978).
[24] S. N. Papadakis *et al.*, J. Opt. Soc. Am. A **7**, 991 (1990).
[25] H. Chen *et al.*, J. Phys.: Condens. Matter **16**, 165 (2004).
[26] Y. L. Geng, X. B. Wu, L. W. Li, and B. R. Guan, Phys. Rev. E **70**, 056609 (2004).
[27] C. W. Qiu, L. W. Li, T. S. Yeo, and S. Zouhdi, Phys. Rev. E **75**, 026609 (2007).
[28] R. E. Colin, Electromagnetics **6**, 183 (2010).
[29] W. Ren, Phys. Rev. E **47**, 664 (1993).
[30] A. N. Oraevsky, Quantum Electron. **32**, 377 (2002).
[31] N. Okada and J. B. Cole, J. Opt. Soc. Am. B **27**, 631 (2010).
[32] D. V. Strekalov, H. G. L. Schwefel, A. A. Savchenkov, A. B. Matsko, L. J. Wang, and N. Yu, Phys. Rev. A **80**, 033810 (2009).

[33] J. M. le Floch *et al.*, Phys. Lett. A **359**, 1 (2007).

[34] J. D. Jackson, *Classical Electrodynamics*, 3rd ed. (Wiley, New York, 1998).

[35] Y. V. Proponenko *et al.*, Tech. Phys. **49**, 459 (2004).

[36] Equation (5) of Ref. [35] contains an error: the expression for $\cos(2\theta)Y_{n,m}(\theta,\varphi)$ is incorrect. Here we report the correct relation, in which the argument of the spherical harmonics is omitted for the sake of simplicity: $\cos(2\theta)Y_{n,m} = A_{n,m}Y_{n+2,m} + B_{n,m}Y_{n-2,m} + C_{n,m}Y_{n,m}$ with $A_{n,m} = 2(n-m+1)(n-m+2)f_nf_{n+1}$, $B_{n,m} = 2(n+m)(n+m+1)f_nf_{f-1}$, and $C_{n,m} = (1-4m^2)/[4n(n+1)-3]$.

[37] *Handbook of Mathematical Functions: With Formulas, Graphs and Mathematical Tables*, edited by M. A. Abramowitz and I. Stegun (Dover, New York, 1965).

[38] I. S. Gradshteyn and I. M. Ryzhik, *Table of Integrals, Series and Products* (Academic, New York, 2007).

[39] To write this equation we have used the expression in Eq. (22) stopped at the order $O[\nu^{-1}]$.

[40] S. Schiller and R. L. Byer, Opt. Lett. **16**, 1138 (1991).

[41] V. S. Ilchenko *et al.*, J. Opt. Soc. Am. A **20**, 157 (2003).

[42] M. Gadtine *et al.*, IEEE Trans. Microwave Theory Tech. **15**, 694 (1997).

[43] B. R. Johnson, J. Opt. Soc. Am. A **10**, 343 (1993).

[44] S. Schiller, Appl. Opt. **32**, 2181 (1993).

[45] C. C. Lam *et al.*, J. Opt. Soc. Am. B **9**, 1585 (1992).

[46] In obtaining the azimuthal component of the quasi-TM magnetic field, the following relation was used: $[\varepsilon_{\theta\theta}\frac{\partial}{\partial\theta} - \varepsilon_{r\theta}\frac{\partial}{\partial r}(r)]\hat{l}_\theta = \hat{l}_\theta[\varepsilon_{\theta\theta}\frac{\partial}{\partial\theta} + \varepsilon_{r\theta}(1 - r\frac{\partial}{\partial r})]$.